

Chapter 2.12 Drying of gases and liquids by activated alumina

Timothy Golden


Studies in Surface Science and Catalysis - STUD SURF SCI CATAL

Cite this paper

Downloaded from [Academia.edu](#) 

[Get the citation in MLA, APA, or Chicago styles](#)

Related papers

[Download a PDF Pack](#) of the best related papers 



[Chap16](#)

Usman Ali Hashmi

[Activated carbon for gas separation and storage](#)

Shivaji Sircar

[Adsorption from theory to practice](#)

louis carton

Chapter 2.12 Drying of gases and liquids by activated alumina

S. Sircar, M. B. Rao and T. C. Golden

Air Products and Chemicals, Inc., 7201 Hamilton Boulevard, Allentown, PA, 18195, USA

1. INTRODUCTION

Removal of trace and bulk water from a fluid (gas or liquid) stream is a major unit operation in the chemical and petrochemical industries [1–3]. The drying process is necessary to (a) prevent condensation and freeze-out of water in plant pipeline and equipment, (b) eliminate corrosion in process equipment, (c) protect against undesirable chemical reactions such as hydration, hydrolysis, etc., (d) prevent catalyst poisoning, and (e) meet product fluid composition specification. Selective adsorption of water on a solid desiccant such as zeolites, silica gels and activated aluminas is often used as the method of drying the fluid stream. Various forms of cyclic pressure swing adsorption (PSA) and thermal swing adsorption (TSA) concepts are generally used as the drying process. These processes utilize regenerative schemes consisting of adsorption and desorption steps so that the adsorbent can be repeatedly used for drying the fluid stream. The design and cost of operation of these processes demand certain properties for adsorption of water by the adsorbent which facilitate the adsorption and desorption steps. Activated aluminas often provide a large spectrum of desirable adsorptive properties for such drying applications. These properties include adsorption equilibria, adsorption kinetics, heats of adsorption, and adsorption and desorption column dynamics which govern the performance of the drying process. This chapter briefly describes these properties for adsorption of water on various forms of alumina and illustrates several conventional drying processes using alumina.

2. PHYSICOCHEMICAL STRUCTURE OF ALUMINA

Most aluminas are produced by precipitation from an aluminate solution using the well-known Bayer process [4]. Numerous stable and transitional forms of alumina can be formed. The thermodynamically stable forms such as alpha alumina are of little use for drying application because of their low surface areas and porosities. The transitional aluminas such as gamma and eta which are formed by thermal dehydration of aluminum hydroxides are mostly used as desiccants. They consist of Al^{+3} and O^{-2} ions bonded in either tetrahedral or octahedral coordination. The resulting crystal structure is cubic or hexagonal closed packed. Generally, the oxygen sublattice is fairly well organized and

the aluminum sublattice is more disordered which actually makes many commercially available aluminas (mainly gamma form) amorphous in nature. A random grouping of aluminum oxides and hydroxides form the structure of the commercial alumina. These can create a large spectrum of micro- and meso pores with surfaces containing both basic (hydroxyl and O^{-2} anion vacancies) and acidic (unsaturated Al^{+3} ions as Lewis and protonated hydroxyl as Brönsted) sites of various strengths and concentrations [4].

The chemical nature of the sites of alumina for water adsorption is not clearly understood. Chemisorption of water through dissociation into H^{+} and OH^{-} ions which attach to the alumina surface, hydrogen bonding of water with surface oxygen and hydroxyl groups, van der Waals and pole-pole interactions between the water molecule and the alumina surface as well as condensation of water vapour in the mesopores of alumina are possible mechanisms [5].

Table 1 lists some of the physical properties of several commercially produced activated aluminas. It shows the available variety of structural properties. These values were obtained from the manufacturer's literature.

Table 1
Physical properties of activated aluminas

	F-1	H-151	AA-300	R-P Grade A	A-201	Actal
Manufacturer	Alcoa USA	Alcoa USA	Alcan Canada	Rhone-Poulenc France	Kaiser USA	Laporte UK
BET Area (m^2/g)	260	350	330	340	350	275
Pore Volume (cm^3/g)	0.40	0.43	0.44	0.40	0.46	0.50
Bulk Density (g/cm^3)	0.85	0.85	0.84	0.77	0.75	0.64
Particle Density (g/cm^3)	1.42	1.38	1.34	—	1.40	1.15
Mean Pore Diameter (Å)	26	43	65	20, 40	52	28

3. ADSORPTION OF WATER VAPOUR FROM GAS STREAMS ON ACTIVATED ALUMINAS

The difference in the pore structure and surface chemistry of different activated aluminas is manifested by significantly different characteristics for adsorption of water vapour as pure gas or from gas mixtures. These properties are illustrated below.

3.1. Equilibrium adsorption of pure water vapour

The isotherms for adsorption of pure water vapour on activated aluminas are typically Type I (microporous) or Type IV (mesoporous) in shape according to the Brunauer classification [6]. Figure 1 shows several examples. Alcoa F-1 alumina has a type I shape while Alcan AA-300 and Alcoa H-156 exhibit type IV shapes. The plots represent the specific amount of water vapour adsorbed (n , g/g) as functions of the relative vapour pressure of water ($x = P/P^s$) at $30^\circ C$. P (atm) is the water vapour pressure over the adsorbent

and $P_s(\text{atm})$ is the saturation vapour pressure of water at 30°C . These data were measured in Air Products laboratories. They demonstrate the substantially different adsorption characteristics of water vapour on different samples of alumina. The specific saturation adsorption capacities of water (m , g/g) by the alumina at the limit of $x \rightarrow 1$ is controlled by the pore volume of the adsorbent. The entire pore volume is filled with liquid water at that limit.

Empirical adsorption equilibrium models like Langmuir and Freundlich can generally be used to describe type I pure water vapour adsorption isotherms on aluminas [6]:

$$n = \frac{mbP}{1 + bP}; \quad b = b_0 e^{q_0/RT} \quad \text{Langmuir:} \quad (1)$$

$$n = CP^k; \quad C = C_0^{kq_0/RT} \quad \text{Freundlich:} \quad (2)$$

where $b(\text{atm}^{-1})$ and $C(\text{atm}^{-k})$ are the Langmuir and Freundlich gas–solid interaction parameters, respectively. They are exponential functions of temperature. q_0 (kJ/mole) is the isosteric heat of adsorption of water vapour on the alumina at the limit of zero water loading ($n \rightarrow 0$). b_0 , C_0 and k are temperature independent constants. T is the temperature of adsorption, P is the equilibrium adsorption pressure and R is the gas constant.

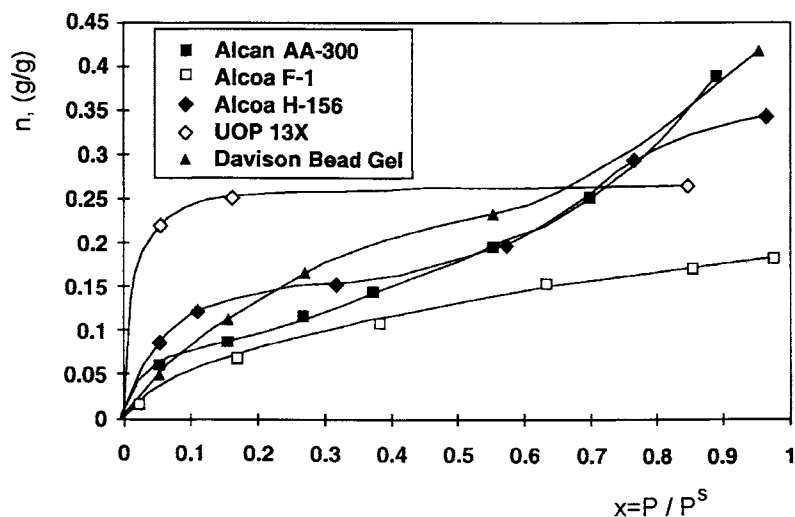


Figure 1. Water vapour isotherms on aluminas, 13X zeolite, and silica gel at 30°C .

Equations (1) and (2) are applicable when the alumina is energetically homogeneous (isosteric heat of adsorption, q , is independent of water loading, n). The Toth equation can be used when the alumina is energetically heterogeneous (q decreases with increasing n) and the isotherm shape is Type I [7]:

$$n = \frac{mbP}{[1 + (bP)^k]^{1/k}}; \quad b = b_0 e^{q_0/RT} \quad \text{Toth:} \quad (3)$$

$k(\leq 1)$ is a temperature dependent heterogeneity parameter.

Both types I and IV isotherms can be described in terms of adsorption (micro and meso pores) and condensation (mesopores only) of water vapour [8]:

$$n = \frac{(V_m/v_L)cx}{1+(c-1)x} + \frac{(S_M \cdot mb)x}{1+(b-1)x}; \quad 0 \leq x \leq x_m \quad (4a)$$

$$n = \frac{(V_m/v_L)cx}{1+(c-1)x} + \frac{2\alpha \bar{V} \Gamma(p, \epsilon_x)}{p \Gamma(p)} \cdot \frac{mbx}{1+(b-1)x} + \left(\frac{\bar{V}}{v_L}\right) \left[\frac{\Gamma(p+1, \epsilon_m) - \Gamma(p+1, \epsilon_x)}{\Gamma(p+1)} \right]; \quad x_m \leq x \leq 1 \quad (4b)$$

where V_m (cc/g) and \bar{V} (cc/g) are, respectively, the micro and total specific pore volumes of the alumina, S_M (cm²/g) is mesopore BET surface area. m (mol/g) is the monolayer capacity for water adsorption on mesopore area and v_L (cc/mol) is the molar volume of liquid water. c and b are, respectively, gas-solid interaction parameters for the micro and meso pores. Parameters α and p describe the pore size distribution (gamma function) of the adsorbent. The condensation in the mesopores is described by the Kelvin model which begins when the water relative vapour pressure is x_m .

Figure 1 also shows the pure water vapour adsorption isotherms on UOP 13X zeolite and a sample of Davison silica gel at 30°C. These data were measured at Air Products' laboratories. They are, respectively, type I and IV in shape. The zeolite adsorbs water very strongly (very high capacity at low x). The water adsorption capacities of the silica gel is comparable to those of the aluminas at low x but it exhibits higher water adsorption capacities at higher values of x . The Henry's law constants [$K = \left(\frac{\partial n}{\partial x}\right)_T$ at $x \rightarrow 0$] for the isotherms of Figure 1 are given in Table 2. The moderate strength of adsorption of water by the aluminas and silica gels make them easier to desorb in a drying process cycle. The aluminas are, however, preferred over silica gels in most practical processes because of their mechanical integrity.

Table 2
Henry's law constants for pure water adsorption on various desiccants

Adsorbent	Henry's law constants (K) at 30°C (g/g)
Alcoa F1	1.1
Alcoa H-156	2.7
Alcan AA-300	2.4
13X Zeolite	140.0
Davison silica gel	1.2

3.2. Heterogeneity of adsorption of water vapour

As mentioned earlier, the alumina surface can be energetically homogeneous or heterogeneous for adsorption of water vapour. The variation in isosteric heat of adsorption (q) with water loading (n) provides a measure of the degree of heterogeneity of the alumina. Figure 2 shows plots of q vs n for three samples of alumina.

The isosteric heat of adsorption exhibits the highest value in the Henry's law region ($x \rightarrow 0$) and then gradually decreases to the heat of vapourization of water (42 KJ/mol) at condensation point ($x \rightarrow 1$). Figure 2 shows that Alcan PSA-I alumina shows a very small variation in q values (relatively homogeneous) over the entire water vapour pressure range while the other two aluminas (RP-Grade A and Alcan AA-300) exhibit large variations (highly heterogeneous) of q values [9]. The comparative isosteric heat of adsorption of water vapour on 13X zeolite is ~ 75 kJ/mol which remains practically constant over the entire range of the water adsorption isotherm. Thus, aluminas require much less energy for desorption.

The isosteric heat of adsorption at a given water loading (n) can be calculated by measuring isotherms at different temperatures [6]:

$$\frac{q(n)}{RT^2} = \left[\frac{\partial \ln P}{\partial T} \right]_n \quad (5)$$

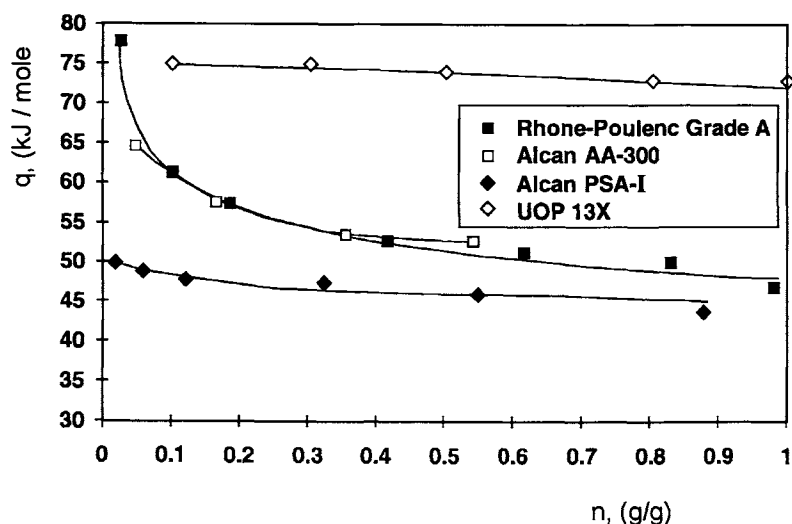


Figure 2. Isosteric heat of adsorption for water vapour on aluminas and 13X zeolite

For the heterogeneous Toth isotherm, q is given as a function of fractional coverage ($\theta = n/m$) by [17]:

$$q = q^0 + \left(\frac{RT^2}{k} \right) \cdot \left(\frac{d \ln k}{dT} \right) \left[\frac{(1 - \theta^k) \ln(1 - \theta^k) + \theta^k \ln \theta^k}{(1 - \theta^k)} \right] \quad (6)$$

q_0 is the isosteric heat of adsorption of water at the limit of zero loading ($\theta \rightarrow 0$).

3.3. Temperature dependence of water adsorption isotherms

Figure 3 shows the isotherms for adsorption of water on Alcan AA-300 at 30 and 70°C.

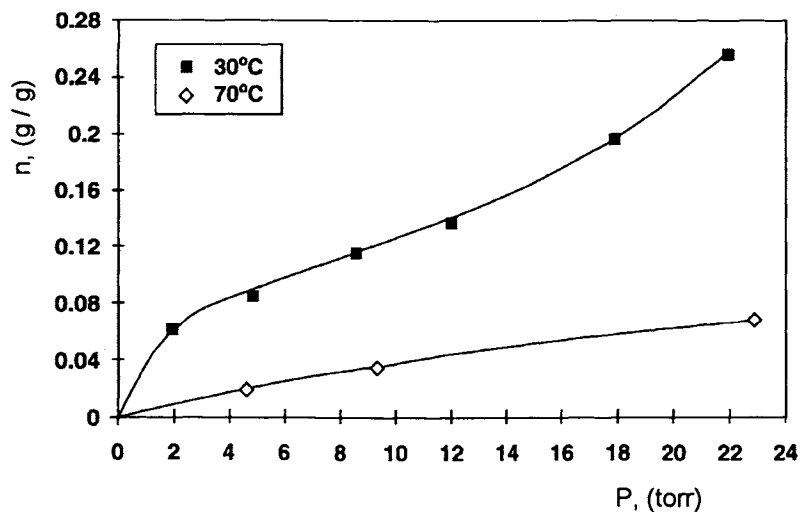


Figure 3. Water vapour isotherms on Alcan AA-300 alumina at 30 and 70°C.

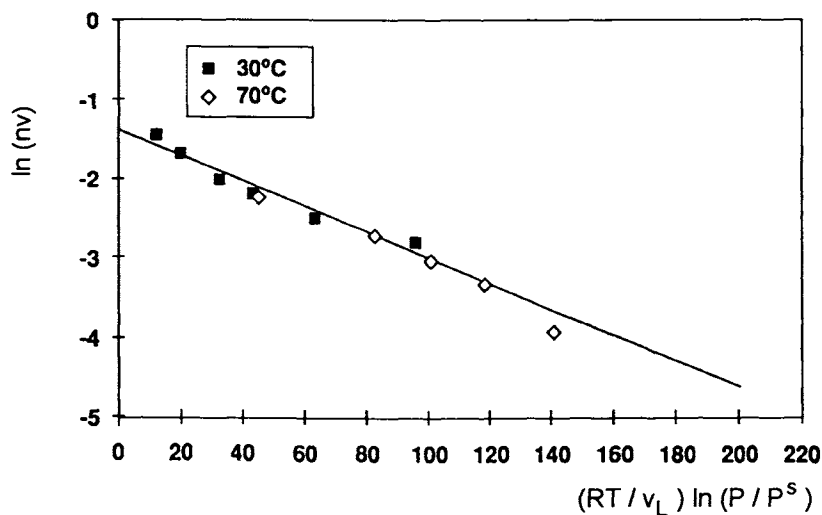


Figure 4. Polanyi potential plot for water vapour adsorption at 30 and 70°C on Alcan AA-300 alumina.

These data were also measured in the Air Products' laboratories. The Polanyi potential concept [6] can be used to coalesce these isotherms at different temperatures into a single

curve as shown by Figure 4. The ordinate of the plot represents the amount of water adsorbed expressed as liquid volume. The abscissa represents the Polanyi potential. The concept can be used to obtain a first pass estimation of temperature dependence of water vapour adsorption on aluminas.

3.4. Adsorption of water vapour from gas mixtures

The selectivity of adsorption ($S = n_1 y_j / n_j y_1$) of water vapour (component 1, mole fraction y_1) on aluminas over component j (mole fraction y_j) of a gas mixture can be complex functions of adsorbate loadings (n_1, n_j), system temperature and pressure. There is a scarcity of published data on water adsorption from multicomponent gas mixtures on alumina. Typically, it is assumed that water is exclusively adsorbed on aluminas ($S \rightarrow \infty, n_j \rightarrow 0$) from non-polar gases such as air or natural gas. The assumption may not be valid when the gas mixture contains polar components. The mixed gas Langmuir or Toth models may be used to describe multicomponent Type I equilibria on aluminas [6,7]. No isotherm model is available to describe adsorption of water from gas mixtures when there is partial condensation of water in the mesopores of the alumina.

3.5. Kinetics of adsorption of water vapour

The kinetics of actual adsorption of water on the sites of alumina is very fast. However, a substantial resistance to mass transport can be exhibited by the finite diffusivity of water molecules from the external gas phase to the adsorption sites through the porous network of the adsorbent particle. Diffusion of water vapour (molecular and Knudsen) through the pores of the alumina particle as well as the surface diffusion of adsorbed water on the pore walls [11-13] can contribute to the overall transport process. The presence of other non-adsorbing or adsorbing components can significantly influence both pore and surface diffusivity values for water. Table 3 shows a family of water vapour diffusivity data on Rhone-Poulenc grade A alumina in presence of N_2 and He as carrier gases at a total gas pressure of 1.0 atmosphere. The water isotherm has a type IV shape [9,11]. Pore diffusion

Table 3
Pore (D_p) and surface diffusivities (D_s) of water vapour on Rhone-Poulenc alumina

Partial pressure of water vapour (Pa)	Carrier gas	Temperature (°C)	D_p (cm^2/s)	D_s (cm^2/s)
59	N_2	24.0	$4.7 \cdot 10^{-2}$	0
		100.0	$6.7 \cdot 10^{-2}$	0
709	N_2	24.0	$4.7 \cdot 10^{-2}$	0
2013	N_2	24.0	$4.7 \cdot 10^{-2}$	$2.9 \cdot 10^{-6}$
2733	N_2	24.0	$4.7 \cdot 10^{-2}$	$2.9 \cdot 10^{-6}$
709	He	24.0	$11.0 \cdot 10^{-2}$	0
		100.0	$13.7 \cdot 10^{-2}$	0
2013	He	24.0	$11.0 \cdot 10^{-2}$	$2.9 \cdot 10^{-6}$

of water dominates the overall transport into the Rhone-Poulenc alumina particles at low water loadings. Surface diffusion of water on pore walls, on the other hand, contribute substantially to overall transport process at high water loadings (x values above the point of inflection of type IV isotherm).

Fickian Diffusion and Linear Driving Force models are generally used to describe the transport of water vapour into the alumina particles. For isothermal adsorption of water vapour from a constant partial pressure (P^0) batch adsorption system on a spherical adsorbent particle of radius R_p , the uptake profiles are given by [13]:

$$\text{Fickian Diffusion (FD):} \quad \frac{m(t)}{m^0} = 1 - \frac{6}{\pi^2} \sum_{n=1}^{\infty} \frac{1}{n^2 \exp(-n^2 \pi^2 D t / R_p^2)} \quad (7)$$

$$\text{Linear Driving Force (LDF):} \quad \frac{m(t)}{m^0} = 1 - e^{-kt} \quad (8)$$

where $m(t)$ is the amount of water adsorbed at time t on an initially clean adsorbent. m^0 is the equilibrium adsorption capacity of water at P^0 and T . D and k are the overall diffusivity or mass transfer coefficient for adsorption of water vapour into the particle. Isothermal uptake measurements, however, may not be feasible due to generation of heat of adsorption [14] and non-isothermal uptake models (FD and LDF) must be used [13,14].

3.6. Column dynamics for ad(de)sorption of water vapour

The dynamics of ad(de)sorption of water vapour from a carrier gas in a packed alumina column is governed by the adsorption equilibria and kinetics for the system. For the adsorption process, a mass transfer zone (MTZ) for water is formed within the column which propagates from the feed gas end to the column exit. The MTZ is generally constant

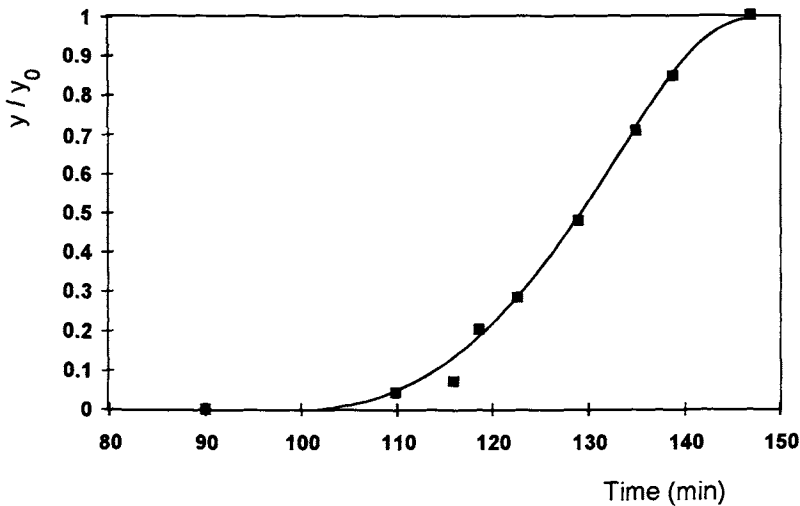


Figure 5. Water breakthrough curve on Alcan AA-300 alumina at 50°C. Feed: 3370 ppm water in N_2 at ambient pressure.

pattern in shape when the water adsorption isotherm is Type I or when the water partial pressure is below the inflection point of a type IV isotherm [13]. Otherwise a proportionate pattern MTZ is formed [13]. Figure 5 shows the constant pattern water breakthrough curve (exit gas water composition vs time) from an Alcan AA-300 column at 50°C where the feed gas contained 3370 ppm of water vapour in nitrogen at atmosphere pressure. These data were measured in Air Products' laboratory. The column remains essentially isothermal when the feed gas water concentration is very dilute. A non-isothermal type I or type II column dynamics is exhibited when the water concentration in feed is moderate [15,16]. Figure 6 shows an example of type II non-isothermal column breakthrough curve from a Laporte alumina at 26.6°C where the feed gas contained an air-water (37% RH) mixture [17].

There is no published data on desorption of water vapour from a column by purging the column with a water free gas. However, such a desorption process produces a proportionate pattern MTZ within the column for a type I adsorption isotherm. The zones are generally governed by local adsorption equilibria within the column [18,19].

The constant pattern water breakthrough curve for isothermal adsorption of trace moisture (Langmuir isotherm) from an inert carrier gas can be described by [15]:

$$(t_2 - t_1) \frac{(1+b)}{b} \cdot k = \frac{1}{\lambda^0} \ln \left[\frac{\phi_2(1-\phi_1)}{\phi_1(1-\phi_2)} \right] + \ln \frac{\phi_1}{\phi_2} \quad (9)$$

where t_i is the time at which the exit gas water molar fraction is given by y_i . ϕ_i is the ratio of y_i to feed gas water molar fraction y_i^0 . $\lambda^0 (= n^0/m)$ is the fractional water loading at the feed gas conditions. b and m are Langmuir parameters. k is the LDF mass transfer coefficient for water.

Analytical equations to describe isothermal proportionate pattern water desorption

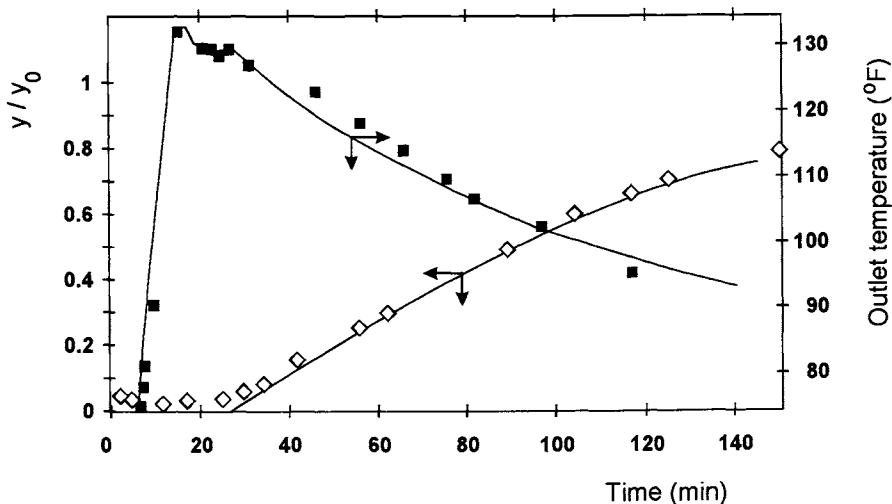


Figure 6. Nonisothermal column breakthrough curve for water (37% R.H.) from air on Laporte alumina at 26.6°C.

characteristics (Langmuir isotherm) by purging the column with an inert carrier gas are also available [19]. They demonstrate that the efficiency of desorption of water by purge is facilitated when the Henry's law constant for water adsorption is low to moderate. Thus, activated aluminas fulfill that requirement.

4. ADSORPTION OF WATER FROM LIQUID STREAMS ON ACTIVATED ALUMINAS

The adsorption of water from a binary or multicomponent liquid mixtures is characteristically different from that from gaseous phase because the pore space within the alumina is always filled with a liquid mixture. Nevertheless, the key characteristics (equilibria, kinetics and ad(de)sorption column dynamics) for adsorption of trace and bulk water from a liquid mixture is very well studied.

4.1. Equilibrium adsorption of trace water from liquid mixtures

The pertinent experimental variable to describe equilibrium adsorption of water from a liquid mixture is the surface excess of water (n_1^e , moles/g):

$$n_1^e = n_1 - [\sum n_j] x_1 \quad (10)$$

where n_1 is the actual specific amount of water (component 1) adsorbed from the mixture (equilibrium bulk phase molar fraction of water = x_1). n_j is the specific amount of component j adsorbed from the mixture [20]. n_1^e is a function of x_1 and the system temperature and it can be directly measured experimentally.

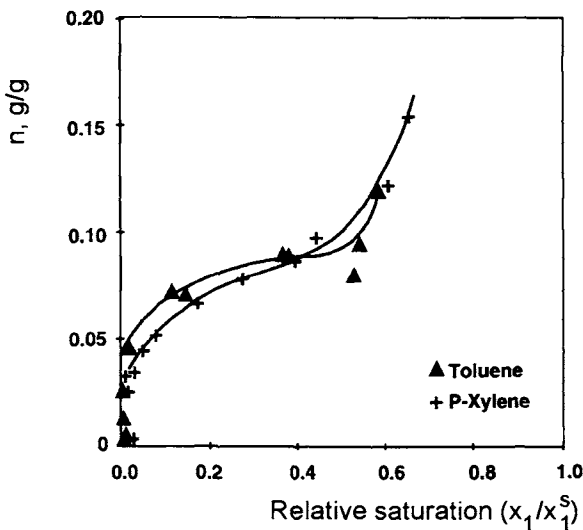


Figure 7. Trace water adsorption isotherms from toluene and p-xylene on Alcoa H-152 alumina at 22°C.

The surface excess isotherm $[n_1^e(x_1)]$ of trace water ($x_1 \ll 1$) from a mixture on activated alumina can have types I and IV shapes analogous to those for adsorption of pure water vapour [20,21].

Figure 7 shows an example of type IV isotherms for adsorption of trace water from toluene and p-xylene mixtures on Alcoa H-152 alumina at 22°C [22]. The abscissa of the plot represents relative saturation of water (x_1/x_1^s), where x_1^s is the molar fraction of water at the solubility limit in the hydrocarbon liquid. Equilibrium isotherm models analogous to those used for pure water vapour adsorption can be derived for describing trace water adsorption from liquid mixtures [20–22].

4.2. Equilibrium adsorption of bulk water from a binary liquid mixture

The surface excess isotherm for adsorption of bulk water ($0 \leq x_1 \leq 1$) from a binary liquid mixture can be ‘U’ (water selectively adsorbed at all values of x_1) or ‘S’ (water not selectively adsorbed at all values of x_1) shaped [20]. Figure 8 shows an example of ‘U’ shaped isotherm for adsorption of water–alcohol binary mixture on Alcoa H-152 alumina

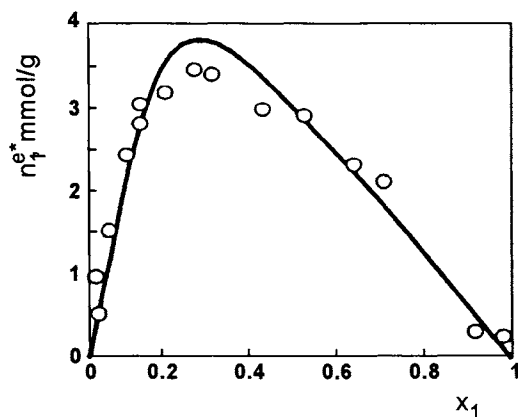


Figure 8. Water–ethanol binary adsorption isotherm on Alcoa H-152 alumina at 30°C.

at 30°C [23]. The monolayer–pore filling (MPF) models can be used to describe these binary isotherms [24,25]:

$$n_1^e = m_1 \frac{[Sa_1x_2 - a_2x_1]}{Sa_1 + \beta a_2} \quad (11)$$

$$S = S_0 [Sa_1 + a_2]^{(\beta-1)/\beta} \quad (12)$$

where m_i is the pore filling capacity of component i . S is the selectivity of adsorption [$S = n_1a_2/n_2a_1$] of water (component 1) over component 2 of the mixture. a_i is the liquid phase activity of component i . $\beta (=m_1/m_2)$ is the size ratio of the two components. S_0 is the selectivity of adsorption water at the limit of $x_1 \rightarrow 0$. Equations (11) and (12) describe

the surface excess isotherm for water on an energetically homogeneous adsorbent. Models are also available to account for energetic heterogeneities of the adsorbent [25].

The effect of temperature on the surface excess isotherms of water from liquid mixtures on the aluminas is generally much less pronounced than those for adsorption from vapours [26].

4.3. Kinetics of adsorption of water from liquid mixtures

The resistance to mass transport for adsorption of water into alumina particles can be governed by diffusion of water molecules through the liquid filled pores as well as by surface diffusion of adsorbed water molecules on the pore walls. A surface excess linear driving force model [SELDF] has been successfully used to describe the adsorption of water from liquid mixtures [27]. For isothermal adsorption of water from a bulk liquid mixture from a constant water composition (x_1^0) batch adsorption system, the uptake profile is given by:

$$\frac{n_1^e(t)}{n_1^{e0}} = 1 - e^{-kt} \quad (13)$$

where $n_1^e(t)$ is the surface excess of water adsorbed at time t on an initially clean adsorbent. n_1^{e0} is the equilibrium surface excess of water at x_1^0 and T . k is the overall mass transfer coefficient for adsorption of water into the adsorbent particle. The kinetics of adsorption of water from liquid mixtures on aluminas are generally orders of magnitude slower than that from gases. Therefore, smaller adsorbent particles are used for liquid drying in order to reduce the transport distance within the adsorbent [27–29].

4.4. Column dynamics for ad(de)sorption of water from liquid mixtures

The dynamics of ad(de)sorption of liquid water from a mixture in packed alumina columns is also governed by the adsorption equilibria and kinetics. For the adsorption process, a MTZ for water is formed within the column which propagates from the feed

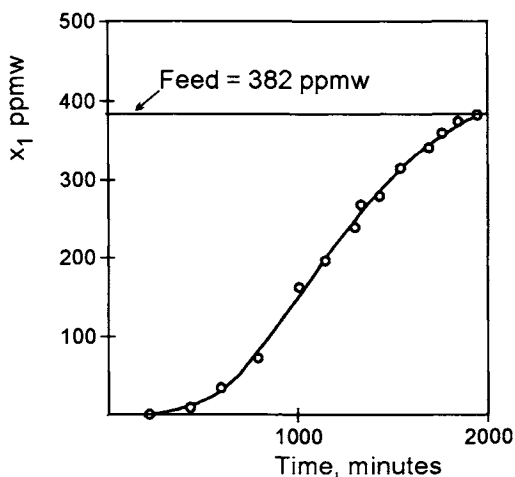


Figure 9. Breakthrough curve for water from p-xylene on Alcoa H-152 alumina at 22°C.

liquid end to the column exit. The MTZ is generally constant pattern [23, 27-29] for an 'U' shaped isotherm (bulk mixture) or for type I isotherm (trace mixture). The column remains nearly isothermal for adsorption from liquid mixtures. Figure 9 shows an example of the MTZ for adsorption of trace water (382 ppm in feed) from p-xylene on H-152 alumina at 22°C [22]. Figure 10 shows an example of the MTZ for adsorption of bulk water (20 molar % in feed = x_1^F) from alcohol on H-152 alumina at 25°C [23]. The ordinate of Figure 10 gives column effluent molar fraction of water (x_1) as a function of total specific quantity of column effluent (Q). The SELDF mass transfer coefficient for this liquid phase system ($k=0.0125$ seconds⁻¹) is much smaller than typical k values of 300 seconds⁻¹ for a gas phase system using the same size adsorbent particles.

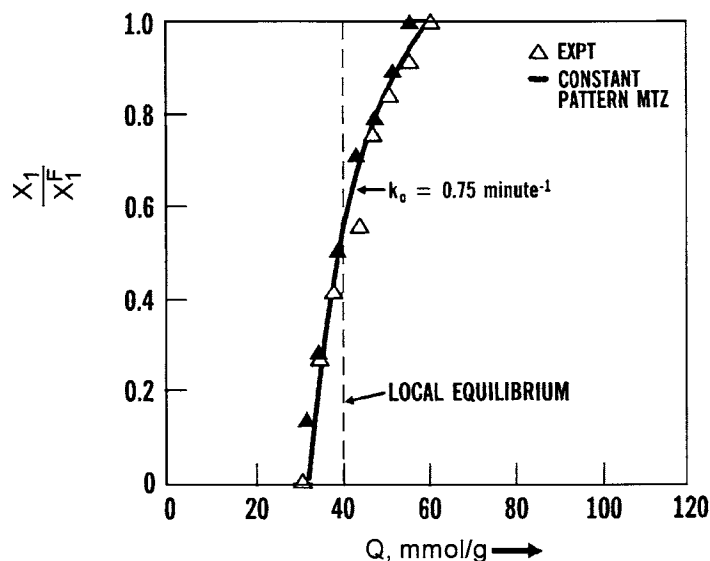


Figure 10. Breakthrough curve for 20 molar % water in ethanol binary liquid mixture on Alcoa H-152 alumina at 25°C.

Analytical mathematical models describing (a) the propagation of constant pattern MTZ and (b) the desorption profiles under local equilibrium conditions in packed columns for ad(de)sorption of bulk binary liquid mixtures having an 'U' shaped surface excess isotherm and obeying SELDF kinetic mechanism are available [27].

5. PROCESSES FOR DRYING OF GASEOUS AND LIQUID MIXTURES

Numerous commercial processes have been developed for dehydration of gaseous mixtures containing trace to dilute amounts of water and for removal of trace to bulk amounts of water from liquid mixtures using activated aluminas as adsorbents. The following sections outline a few of these processes.

5.1. Thermal swing adsorption (TSA) processes for removal of trace water from gases and liquids

The basic concept of a TSA drying process consists of (a) selective adsorption of trace or dilute water from the contaminated fluid mixture by flowing the fluid over a packed column of alumina particles while withdrawing a dry product stream until the water concentration at the column effluent rises to a predetermined value and then (b) thermal desorption of the adsorbed water by heating the column with a relatively dry fluid stream. The adsorbent is repeatedly used in a cyclic manner by carrying out steps (a) and (b). More than one adsorbent column is required for continuous processing of the wet feed fluid stream and production of a dry fluid stream.

The adsorbent column is generally regenerated immediately after the adsorption step when the feed stream is a gaseous mixture. In addition, the adsorbent column is usually drained to remove inter-particle liquids before regeneration begins, when the feed stream is a liquid mixture.

Many different regeneration options are practiced [30–34]. For example, a portion of the dry product gas can be used to provide for the regeneration gas. Figure 11 is a schematic flow diagram for a three column TSA gas drying system. The dry regenerated gas is passed through one column (which has completed heating step) in order to cool the column. The effluent from that column is heated and passed through another column (which has completed adsorption step) for desorption of water. The third column (which has completed cooling step) is used to remove water from fresh feed. Hot wet feed gas can also be used for regeneration [30]. The temperature range of regeneration for the activated aluminas is 200–300°C and the quantity of regenerating gas is 10–15% of feed gas processed. Higher regeneration temperatures are used when more stringent drying is required. For example, a 200°C regeneration is sufficient when the water concentration of effluent product gas is about 10 ppm. A 300°C regeneration reduces the product gas water concentration to below 1 ppm.

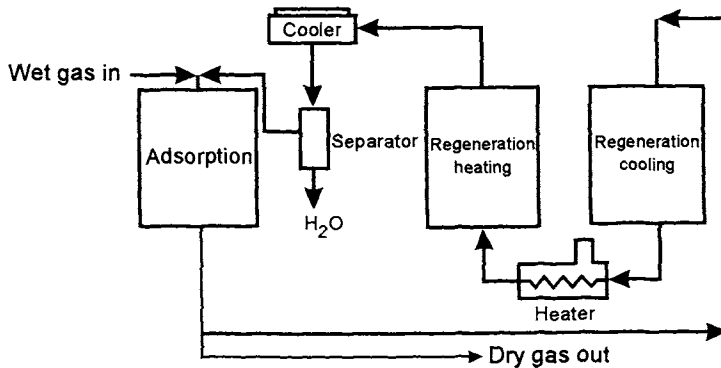


Figure 11. Schematic flow diagram for three column thermal swing adsorption system for gas drying.

Figure 12 is a schematic flow diagram for a two column liquid phase TSA drying system where trace water is removed from a hydrocarbon stream [31]. An external regeneration

gas is used in this scheme. The hot effluent gas during the regeneration step is cooled and condensed to form a two phase immiscible liquid mixture. The hydrocarbon-rich phase is recycled to the TSA system by mixing it with the fresh feed stream while the water-rich phase is rejected.

The dynamic desiccant capacity of the alumina in a TSA process depends on the type of alumina, nature and composition of the feed stream, regeneration temperature, etc. A typical water removal capacity for alumina is 5–15% by weight. The typical total cycle time for a TSA process is 2–8 hours.

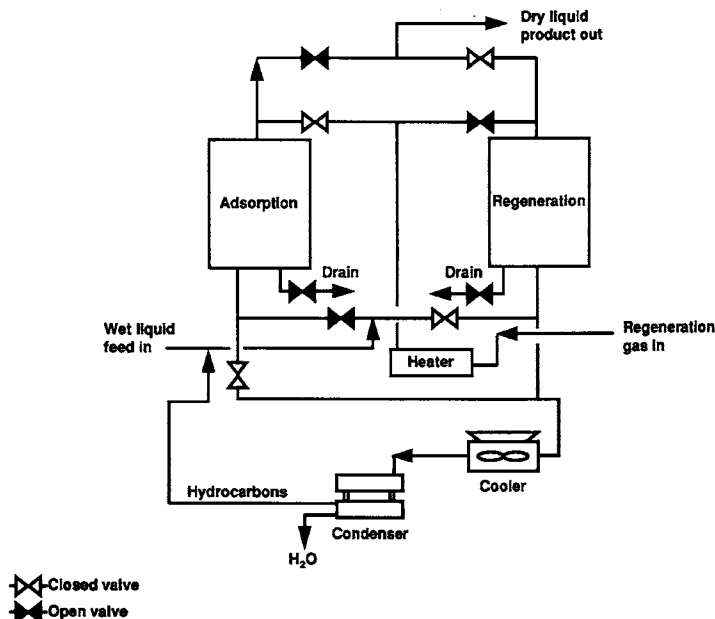


Figure 12. Schematic flow diagram for two column thermal swing adsorption system for liquid drying.

5.2. Pressure swing adsorption (PSA) process for removal of trace water from gases

The basic concept of a PSA drying process consists of (a) selective adsorption of trace or dilute water from the contaminated gas at a relatively high (50–100 psig) total gas pressure by flowing the gas over a packed bed of alumina particles while withdrawing a dry product gas stream until the water concentration at the column effluent rises to a predetermined level and then (b) desorption of the adsorbed water from the alumina by lowering the superincumbent partial pressure of the water in the column. Again the adsorbent is repeatedly used in a cyclic manner by carrying out steps (a) and (b). The desorption in a PSA process is achieved by (a) lowering the total gas pressure of the column to near ambient (depressurization) and by (b) flowing a portion of the dry product gas over the column at near ambient pressure (purge). Adsorption at a relatively low pressure (5–10 psig) and desorption under vacuum (both depressurization and purge) are also

possible options [33–36].

Figure 13 is a schematic flow diagram for a two column Skarstrom type [36] PSA drier. The process can be used to obtain very dry product gas ($< -60^{\circ}\text{C}$ dew point). The product purity depends on the type of alumina used, feed gas pressure and dry purge gas quantity. Typically a practical PSA drier uses 15–30% of product gas as purge. The typical total cycle time for a PSA process is 2–4 minutes.

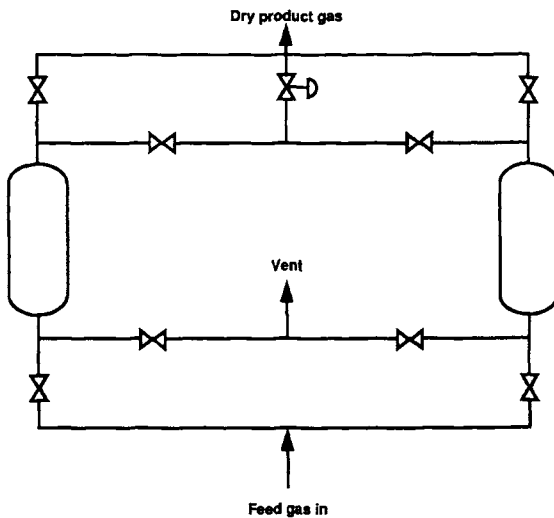


Figure 13. Schematic flow diagram for two column Skarstrom pressure swing adsorption cycle for gas drying.

5.3. Concentration swing adsorption (CSA) and concentration–thermal swing adsorption (CTSA) processes for drying bulk liquid mixtures

Removal of bulk water from liquid mixtures by adsorption require different processing concepts. Novel CSA and CTSA concepts are developed [23,28,29] where the adsorption step is carried out by flowing the wet bulk liquid mixture through a packed column of alumina in order to produce a dry product liquid stream. The less selectively adsorbed components of the liquid mixture are then removed from the column (from the intra- and inter-particle void space) by rinsing the column with pure water. The water saturated column is then subjected to the desorption step by flowing an extraneous non-adsorbing liquid stream or by thermally heating with a relatively dry extraneous gas stream. The column is drained to remove inter-particle water prior to thermal regeneration.

Figure 14 shows a schematic flow diagram of a CTSA drying process for bulk liquid mixture where dry air produced by a PSA drier is used to heat the liquid drying columns.

5.4. Design of TSA and PSA drying processes

The design of practical TSA and PSA processes often require bench or pilot scale operational data because of the lack of quantitative methods for estimation of multicomponent

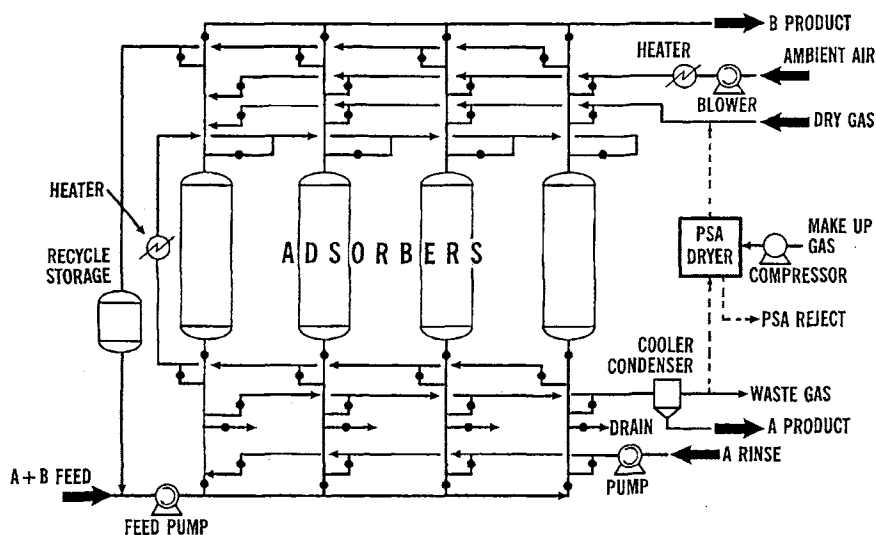


Figure 14. Schematic flow diagram for concentration-thermal swing adsorption system for bulk liquid drying.

gas and liquid adsorption equilibria, kinetics and column dynamics [37]. Mathematical models of these processes are often very useful for scale up and optimization. These models require simultaneous solutions of mass, heat and momentum balance equations (partial differential equations) describing the ad(de)sorption processes within the columns. The equations are solved using appropriate initial and boundary conditions for each step of the process. Multicomponent adsorption equilibria, heat and kinetics constitute the key input variables for the solutions of the models. Manufacturers of commercial drying (gas and liquid) process systems have developed several practical short-cut design procedures [30-36].

6. CONCLUSION

Drying of gases and liquids by activated alumina is a very flexible and versatile process concept. A large variety of synthetic alumina structures having a range of properties for adsorption water from various gases and liquids is commercially available. Numerous PSA, TSA and CSA process concepts have been designed to remove trace or bulk water from gaseous and liquid streams.

REFERENCES

1. D. Basmadjian, The Adsorption Drying of Gases and Liquids, Chapter 8 (pp 307-357) in: *Advances in Drying*, vol. 3 (1984).
2. G. Keller, R. A. Anderson and C. M. Yon, *Adsorption*, Chapter 12 (pp 644-696)

- in: Handbook of Separation Process and Technology, R. W. Rousseau (ed.), John Wiley and Sons, New York (1987).
3. A. L. Kohl and F. C. Riesenfeld, Gas Dehydration and Purification, Chapter 12 (pp 574–656), in: Gas Purification, Gulf Publishing Co., Houston (1979).
 4. K. P. Goodboy and H. L. Fleming, Chem. Eng. Prog., (1984) 63.
 5. H. Knozinger and P. Ratnasamy, Cat. Rev. Sci. Eng., 17 (1978) 31.
 6. D. M. Young and A. D. Crowell, Physical Adsorption of Gases, Butterworths, London, 1962.
 7. M. Jaroniec and J. Toth, J. Colloid Polym. Sci., 254 (1976) 643.
 8. S. Sircar, Carbon, 25 (1987) 39.
 9. R. Desai, M. Hussain and D. M. Ruthven, Can. J. Chem. Eng., 70 (1992) 699.
 10. S. Sircar, Langmuir, 7 (1991) 3065.
 11. R. Desai, M. Hussain and D. M. Ruthven, Can. J. Chem. Eng., 70 (1992) 707.
 12. L. Marcussen, Chem. Eng. Sci., 29 (1974) 1061.
 13. D. M. Ruthven, Principles of Adsorption and Adsorption Processes, John Wiley and Sons, New York, 1984.
 14. S. Sircar, J. Chem. Soc. Faraday Trans. I., 79 (1983) 785.
 15. S. Sircar and R. Kumar, I&EC Process Des. Dev., 22 (1983) 271.
 16. C. L. Chou, Chem. Eng. Communications, 36 (1987) 211.
 17. J. W. Carter and D. J. Barrett, Trans. Inst. Chem. Engrs., 51 (1973) 75.
 18. S. Sircar and R. Kumar, I&EC Process Des. Dev., 24 (1985) 358.
 19. S. Sircar and T. C. Golden, I&EC Research, in press.
 20. J. J. Kipling, Adsorption from Solutions of Non-Electrolytes, Academic Press, New York, 1965.
 21. S. Sircar, A. L. Myers and M. C. Molstad, Trans Faraday Soc., 66 (1970) 2354.
 22. S. Joshi and J. R. Fair, Ind. Eng. Chem., 30 (1991) 177.
 23. M. B. Rao and S. Sircar, Adsorption Sci. Tech., 10 (1993) 93.
 24. S. Sircar, Surf. Sci., 148 (1984) 478.
 25. S. Sircar, Surf. Sci., 148 (1984) 489.
 26. S. Sircar, I&EC Research, 32 (1993) 2430.
 27. S. Sircar and M. B. Rao, AIChE J., 38 (1992) 811.
 28. M. B. Rao and S. Sircar, Sep. Sci. Tech., 27 (1992) 1875.
 29. M. B. Rao and S. Sircar, Sep. Sci. Tech., 28 (1993) 1837.
 30. Trade Publication (F35-14480), Choosing an Alcoa Activated Alumina Desiccant Basics of Dehydration Design, Alcoa, Pittsburgh, Pennsylvania, U.S.A., 15219.
 31. Trade Publication (F35-14481), Dehydrating Liquids With Alcoa Activated Aluminas, Alcoa, Pittsburgh, Pennsylvania, U.S.A., 15219.
 32. Trade Publication, Activated Alumina, Rhone-Poulenc, Paris, France.
 33. Trade Publication (IC-117R 2500), Improve Your Gas Drying Operations, Kaiser Chemicals, Oakland, California, U.S.A. 94643.
 34. D. H. White, Selecting the Right Desiccant Dryer, Machine Design, 2 (1985).
 35. Trade Publication, Drying with Harshaw Activated Aluminas, Harshaw Chemical Company, Cleveland, Ohio, U.S.A. 44106.
 36. C. W. Skarstrom, U. S. Patent 2,944,627 (1960).
 37. S. Sircar, Proceedings of Third International Conference on Fundamentals of Adsorption, Sonthofen, Germany, pp 815–843 (1991).